Development and optimization of a rat Purkinje neuron culture to study paraneoplastic cerebellar degeneration

Ida Margrethe Uggerud
UiB: Universitetet i Bergen
Torbjorn Krakenes
UIB: Universitetet i Bergen
Hirokazu Hirai
Gunma University Graduate School of Medicine School of Medicine Faculty of Medicine: Gunma Daigaku Daigakuin Igakukei Kenkyuka Igakubu
Christian Alexander Vedeler
Haukeland University Hospital: Haukeland Universitetssjukehus
Manja Schubert (schubert_manja@hotmail.com)
Haukeland University Hospital: Haukeland Universitetssjukehus https://orcid.org/0000-0003-3592-2470

Research Article

Keywords: in vitro culture system, paraneoplastic cerebellar degeneration, Purkinje neuron, Yo antibodies

Posted Date: April 6th, 2022

DOI: https://doi.org/10.21203/rs.3.rs-1505572/v1

Abstract

Background: Elucidation of the mechanisms involved in neurodegenerative disease has been hampered by the lack of robust cellular models that replicate *in vivo* features.

Methods: We developed a refined protocol for generation of age-dependent, well-developed, and synaptically active rat Purkinje neurons in a multilayer cell network culture that can be used to study neurodegenerative diseases such as paraneoplastic cerebellar degeneration (PCD).

Result: Independent of the age of the tissue from which the culture was driven, the properties of the generated rat Purkinje neuron culture are complex and robust, allowing great experimental flexibility. Using our model, we found that the application of Yo antibodies, which are associated with PCD, alters the structure of the dendritic arbour of cultured Purkinje neurons within 48h. The numbers of dendrites per branch-order, the branch-order in itself, and the dendritic length were reduced by treatment with anti-Yo.

Conclusion: The here presented *in vitro* model is flexible and can be used to investigate disease mechanisms that disturb Purkinje neuron function and communication in a multilayer network. It proved that anti-Yo has a functional role in the pathogenesis of PCD.

Background

In patients with immune-mediated paraneoplastic syndromes, neuronal loss occurs quickly, and treatment is limited because the mechanisms of pathology remain unclear [1]. Unravelling thus mechanisms depends on the availability of robust and flexible disease models that provide insight at both the single-cell level and network levels. One of the most common paraneoplastic neurological syndrome is paraneoplastic cerebellar degeneration (PCD), a disease associated with ovarian and breast cancer, in which the loss of Purkinje neurons (PNs) is hypothesized to result due to cross-reactivity of Yo antibodies that bind to CDR2/2L [2,3]. For this disease, there is no mouse or rat *in vivo* model, but there is a well-established rat *in vitro* model, the PCD model of organotypic slice culture [2,4,5]. Neuronal culture systems are very valuable for study of basic principles of the nervous system, however, each system has its advantages and disadvantages. Organotypic slice cultures provide an intact neuronal network, but single-cell studies, genetic modifications, and long-term studies are difficult or impossible with these models. Dissociated neuronal cultures allow manipulations and observations of neurons on the single-cell level, but quality and survival of the cultured cells depend on several factors such as animal species, age of tissue used to derive single cells, the surface onto which the single cells are seeded and cultured, and co-factors that drive neuronal growth and development. To date, the majority of successful PN culture models have used embryonic mouse cerebelli. It has proven more difficult to culture and manipulate cells from rats [6], but rats are physiologically, immunologically, genetically, and morphologically closer to humans than are mice [7]. Furthermore, outbred or transgenic rat models [8–10] mimic human neurodegenerative disease mechanisms and progressions more closely than mouse models do [11,12].

Since neurodegeneration generally occurs in the adult or aged human brain, a dissociated culture system derived from mature rather than embryonic tissue is desirable. However, previous attempts to culture functional dissociated neurons from late postnatal and adult tissue have largely been unsuccessful. Our goal was, therefore, to develop a culture protocol that provided mature and synaptically active rat PNs. The protocol described results in a multilayer culture of PNs that are well-developed, mature, and functional and does not dependent on the age of the tissue used to derive these cells. As proof of concept, we studied the effects of PCD associated Yo antibodies on these cultured PNs.

Materials And Methods

Neuronal culture preparation

All procedures were performed according to the National Institutes of Health Guidelines for the Care and Use of Laboratory Animals Norway (FOTS 20135149/20157494/20170001). Wistar Hannover GLAST rat pups (n = 328), embryonic day 18 (E18) to postnatal day 10 (P10), were used for neuronal culture preparation. Briefly, following anaesthesia and decapitation, the brains were rapidly transferred into ice cold EBSS (Gibco, #24010043) solution containing 0.5% glucose (Sigma, #G8769) and 10 mM HEPES (Gibco, #15630056). Under a dissection microscope, the meninges and medulla oblongata were carefully removed, and the cerebellum was separated from the pons and the midbrain. Depending on the culture, either only the cerebellum or the cerebellum including pones was transferred to a 15 mL tube containing 20 U/mL papain (Worthington, #LK003178) dissolved in preparation solution and warmed up to 36 °C. The tube containing the cerebellar tissue was placed into the incubator for 15 minutes at 36 °C with occasionally swirling to digest the tissue. The papain solution was carefully removed with a fire-polished Pasteur, and the digestion reaction was stopped by addition of stop media (advanced DMEM/F12 solution (Gibco, #12634010) containing 0.5% glucose (Sigma, #G8769) and 10% foetal bovine serum (FBS, Gibco, #10500064) pre-warmed

36 °C. After 5 minutes of deactivation, the stop media was removed and 250 µL growth media containing 10% FBS per cerebellum was added. The tissue/media suspension was pipetted up and down with a fire polished Pasteur pipette at least 100 times until cells were separated.

Support cell layer

To prepare the support cell layer, 375.000 cells/mL from cerebellum including pones were seeded on cover slides from Neuvitro (#GG-12-1.5-PDL, 24 well, 500 µL/well; #GG-18-1.5-PDL, 12 well, 1 mL/well; #GG-25-1.5-laminin, 6 well, 2 mL/well) that were pre-coated with poly-D-lysine (PDL) alone or additionally with laminin. Cultures were maintained in 6-, 12-, or 24-well plates in growth media consisting of 45% advanced DMEM/F12 solution (Gibco, # 126340010), 45% NBM solution (Miltenyibiotec, #130-093-570), 1.5% B-27 serum-free supplement (Gibco, #17504044), 1.5% NB-21 serum-free supplement (Miltenyibiotec, #130-093-566), 1% sodium pyruvate (Invitrogen, #11360088), 1% heat-inactivated FBS (Invitrogen, #10500064), 2% Glutamax (Gibco, #35050038), 5 mg/mL D-glucose and 10 mM HEPES (Invitrogen, #15630056) at 36°C. Half of the culture medium was replaced every 7 days.

PN layer

E18- and P0-derived PN cultures were prepared by seeding 500.000 cells/mL from cerebellum without pones onto the support cell layer of different *in vitro* ages. P10-derived PN culture was prepared by seeding 750.000 cells/mL from the vermis of the cerebellum onto the support cell layer of different *in vitro* ages. The growth media was supplemented with insulin (Invitrogen, #12585014; 1:250, stock 4 mg/mL), progesterone (Sigma, #P8783, 1:2000, stock 80 mM), insulin-like growth factor 1 (IGF1; Promokine, #E-60840, 1:40000, stock 1 µg/µL) and Protein kinase C inhibitor K252a (Alomone, # K-150; IC_{50} 25 nM). In long-term cultures that were maintained for more than 28 days *in vitro* the IGF1 and progesterone concentration were reduced to 10 ng/mL and 20 µM, respectively. K252a was supplemented for 21 days before the washout process started, its optimal concentration was experimental evaluated for each tested culture type. Half of the culture medium was replaced every 3.5 days for 6-well plates and every 2 days for 12- and 24-well plates. All experiments testing the yield of PNs from tissue from rats of different ages, different *in vitro* ages of the support cell layers, and K252a concentration were performed randomly, containing 3 to 6 probes per experimental setting and 5 independently repeats for each group and condition.

Lentiviral gene editing

The full-length L7 promoter region (1005 bp) was custom cloned by SBI System Bioscience into construct pCDH-L7-MCS-copGFP (#CS970S-1), and viral particles with a yield of 2.24 x 10^9 ifus/mL were produced. Freshly prepared PNs of E18 or P0 cerebellum suspended in growth media containing no serum were incubated for 10 minutes at 37 °C with 1.22 x 10^6 viral particles/mL before seeding onto the supplement structure layer containing coverslip or live-cell imaging 35 mm µ-dish (Ibidi, #80136). Media was changed after 3 days, and transfection efficiency evaluated by live-cell imaging microscopy at 24 hours post transfection and then daily up to 21 days and weekly up to 169 days in culture, respectively. Lentiviral transfections of PNs in culture were performed 1 day after feeding at 15 days *in vitro* (DIV) and DIV29 by applying 2.5 x 10^6 viral particles/mL. The neuronal development of the GFP-expressing PNs was followed by obtaining 10 independent 3x3 tile scan using the Zyla camera configuration of 2048x2048 with the CFI Plan Apochromat Lambda dry objective 10x0.45 (pixel size 603 nm) or 20x0.75 (pixel size 301 nm) at the Andor Dragonfly microscope system (Oxford Instruments company). Experiments were repeated three times.

Immunohistochemical characterisation of cell types

To evaluate PN yield, the distribution ratios of other cell types of the cerebellum, and their synaptic interactions, cultures were washed with pre-warmed 0.1 M PBS (Gibco, #70013016) and fixed with 1.5-4% paraformaldehyde (PFA, pH 6-7.2; ThermoScientific, #28908) containing 0.5% sucrose for 15 minutes at 36 °C. Tris-based or citric acid-based heat-induced antigen retrieval (pH 9 and pH 6, respectively; 45 min, 85 °C) [13] was perform when necessary (see Table 1). Cultures were quenched with 1xPBS containing 50 mM NH_4Cl (PBS_N), permeabilised with 0.2% Triton X-100 (Sigma, #T9284) in PBS_N (5 min, 36°C), rinsed with PBS_N containing 0.5% cold water fish gelatine (Sigma, #G7041) (PBS_{NG}, 3x15 min), and incubated with primary antibodies over-night at 4°C in PBS_{NG} containing 10% Sea Block (ThermoScientific, #37527), 0.05% Triton X-100 and 100 µM glycine (Sigma, #G7126) to visualise the different cerebellar cell types, including Purkinje neurons and their synaptic interactions (Table 1). The coverslips were rinsed with PBS_{NG} (3x20 min) and incubated with highly cross-absorbed donkey

secondary antibodies conjugated to CF^{TM}488/594/647-Dye (Biotium, #20014, #20115, #20046, #20015, #20152, #20047, #20074, #20075, #20169, #20170; 1:400) for 2 hours at 22°C in PBS_{NG} containing 2.5% Sea Block. To remove unbound secondary antibody, coverslips were rinsed with PBS_N (3x20 min), and briefly dipped into MilliQ water before mounted in hardening Prolong^{TM} Glass Antifade Reagent (Invitrogen, #P36981) onto cover slides. After 2 days of hardening at 18-21°C in the dark, cover slides were stored at 4 °C until imaging.

PN counting and imaging

PNs were counted manually and blind by screening the coverslips using a Leitz Diaplan fluorescence microscope equipped with CoolLED pE-300white lamp. For dendritic tree branch analysis and determination of maturity and synaptic interaction, 10 Z-stack images per cover slide were collected in five independent and randomized experiments at 0.5-1 µm intervals with the Zyla camera configuration (2048x2048) using the the Andor Dragonfly microscope system equipped with a CFI Plan Apochromat Lambda S LWD 40x1.14 water objective (pixel size 151 nm), a 60x1.20 oil objective (pixel size 103 nm), or a CFI SR HP Apo TIRF 100x1.49 oil objective (pixel size 60 nm) to detect DAPI and CF^{TM}488/594/647 dye emission. Stacks were superimposed with Fusion software (Oxford Instruments). 3D surface visualization of synapses was performed using Oxford Instruments analysis software IMARIS 9.3.1 and the filament tracer tool [14].

Dendritic tree branch analysis

The PN dendritic tree development was evaluated by analysing 10 group-dependent PNs per experiment in 10 independent experiments. The order and length of the dendritic arbours was determined using an open-source ImageJ and Fiji plugin Simple_Neurit_Tracer (Neuroanatomy) [15].

Micro-electrode array (MEA) recordings

Primary cultures of E18-derived PNs at a concentration of 500.000 cells/mL were plated onto PDL precoated 24 well format plates of the Multiwell-MEA-system (Multi Channel System-MCS, Reutlingen, Germany). Each well contains 12 PEDOT coated gold micro-electrodes (30 µm diameter, 300 µm space, 3 x 4 geometrical layout) on glass base to facilitate visual checking (Multi Channel System-MCS, #890850, 24W300/30G-288). The amplifier (data resolution: 24 bit; bandwidth: 0.1 Hz to 10 kHz, modifiable via software; default 1 Hz to 3.5 kHz; sampling frequency per channel: 50 kHz or lower, software controlled; input voltage range: ± 2500 mV), stimulator (current stimulation: max. ± 1 mA; voltage stimulation: max. ± 10 V; stimulation pattern: pulse or burst stimulation sites freely selectable) and heating element (regulation: ± 0.1 °C) were integrated into the Multiwell-MEA-headstage which is driven by the MCS-Interface Board 3.0 Multiboot. The Multiwell recording platform was covered by a mini incubator to provide 5% CO_2 and balanced air. Electrophysiological signals were acquired at a sampling rate of 20kHz through the commercial software Multiwell-Screen. Plates were tested every second day from day 5 *in vitro* for spontaneous activity. Raw voltage traces were recorded for 120 seconds, saved, and analysed using offline MCS-Multiwell-Analyzer to calculate spike rate and burst activity, including network properties. Two experimental settings were tested: First, spontaneous spike activity was recorded in PN culture media (45% advanced DMEM/F12 solution, 45% NBM solution, 1.5% B-27 serum-free supplement, 1.5% NB-21 serum-free supplement, 1% sodium pyruvate, 1% heat-inactivated FBS, 2% Glutamax, 5 mg/mL D-glucose, 10 mM HEPES, 16 µg/mL insulin, 25 ng/mL IGF1, 40 µM progesterone, 5 nM K252a) for 63 days. Second, spontaneous spike activity was recorded for the first 28 days in PN culture media that was then exchanged to previously described organotypic brain slice culture media [2] (30% advanced DMEM/F12 solution, 20% MEM solution (Gibco, #41090028), 25% EBSS solution (Gibco, #24010043), 25% heat-inactivated horse serum (Sigma, #H1138), 2% GLUTAMAX, 5 mg/ml D-glucose and 2% B-27 serum-free supplement) for the remaining 45 days of the experiment.

Patient sera

Sera were obtained from two untreated patients with gynecological cancer and PCD who had Yo antibodies against CDR2 and CDR2L (anti-Yo_1 and anti-Yo_2) but lacked antibodies to P/Q-type voltage-gated calcium channel (VGCC) proteins [2]. A pool of sera from 100 healthy age-matched donors (non-$hCDR_{100p}$) was used as a control. Sera were not heat-inactivated before use. The sera were stored at the PND Biobank #133/2015 or the Biobank for diagnostic cancer marker #188.05 with approval of the regional ethics committee, Western-Norway.

In vitro PCD model

Twenty-eight days post-seeding, the culture medium was replaced with medium containing 4 µL/mL human serum positive for Yo antibodies. PN culture was collected 2 or 4 days after commencement of treatment to evaluate the antibody effects. Each independent experiment included treatment (anti-Yo_1 and anti-Yo_2) and positive (non-$hCDR_{100p}$) control to account for variations in cell survival between culture preparations. All treatments were performed in triplicate and five PNs were analyzed per sample.

Results

Rat PN culture: Monolayer versus multilayer culture

To establish a stable and flexible *in vitro* culture PCD model using rat PNs, we first determined which extracellular matrix was needed for maximal neuron growth and survival. Initial attempts to grow PNs directly as a monolayer on glass coverslips coated with PDL, or with PDL and the extracellular matrix protein laminin failed. The yield of PNs per coverslip was minimal or declined to zero after 21 days *in vitro*, respectively; the yield was dependent on the age of the tissue used to derive the neurons (Figure 1a).

We reasoned that other cerebellar cell types might be needed to provide a network structure and paracrine factors critical for PN growth; therefore, we developed a multilayer approach by first plating a support cell layer derived from cerebellum of E18, P0 or P10 rats onto PDL-coated coverslips. We then plated a second cell layer 7 to 48 days later than the first on thus support cell layer. We found that the tissue age of cells used to grow the support cell layer (E18 to P10) had no impact on the PN yield of the second layer; however, the survival rate of the neurons in the second layer did depend on how long the support layer was cultured. The highest survival rate was observed when plated onto the support cell layer for E18-derived PNs at DIV14; for P0-derived PNs at DIV21 and for P10-derived-PNs at DIV28 (Figure 1b).

The use of a support cell layer was associated with higher metabolic demand than single layer cultures and led to non-physiological pH fluctuations. This was associated with increased cell death when half of the culture media was replaced once a week. By decreasing the interval und replacing the culture media either every 3.5-days for 6-well plates or every 2 days for 12- and 24-well plates, pathological pH fluctuations were minimized and a healthy well-developed neuronal network was obtained. Despite these improvements, PN dendritic morphology was poorly developed compared to that *in vivo.* The E18- and P0-derived PNs had fewer and shorter branches than do those derived from P10 rats or *in vivo* (Figure 1c).

Dendritic tree development: importance of paracrine factors and PKC

Next, we examined the effects of supplementing the multilayer culture with paracrine factors, such as progesterone, insulin and IGF1. Supplementation with 40 µM progesterone led to increasingly branched dendritic trees in E18-derived PNs, but had no impact on the branch structures of P0- and P10-derived PNs (Figure 1d). The supplementation with insulin and IGF1 did not improve the branch development but resulted the long-term growth of the other cerebellar cell types including granule, Golgi, Lugaro, unipolar brush, stellate, and basket cells in the multilayer culture (Figure 1e).

As progesterone showed no improvement of the dendritic tree in P0- and P10-derived PNs, we also evaluated the impact of protein kinase C as it is known to be important for long-term anatomical maturation of the PN dendritic tree [16]. Inhibition of the activities of calcium-dependent PKC subtypes using K252a improved dendritic branching of E18- and P0-derived PNs but had no effect on the branching characteristics of P10-derived PNs (Figure 1f-g). Interestingly, PKC inhibition induced by K252a significantly improved cell survival of P0- and particularly of P10-derived PNs in a concentration-dependent manner (Figure 1h). The survival rate in P0-derived PNs was improved by a factor of 6 by blocking 20 % of PKC activity with 10 nM K252a, whereas in P10-derived PN cultures blocking 50% of the PKC activity with 25 nM K252a increased the survival rate by a factor of 28. Inhibiting PKC activity had no effect on the survival rate of E18-derived PNs (Figure 1h).

These observations led to an optimized protocol that archived a well-developed PN enriched layer. The tree main factors that had to be considered were IGF1, progesterone and K252a. The following administration strategy was determined for the enriched PN layer: from DIV1-10 the K252a concentration in the culture was 5 nM for E18-derived PNs, 10 nM for P0-derived PNs and 25 nM for P10-derived PNs. At DIV10 the K252a concentration was raised to 25 nM for all groups to obtain a well-developed and mature dendritic tree until DIV22. From DIV22 the washout phase of K252a started (DIV22-24: 12.5 nM, DIV24-26: 6.75 nM, DIV26-28: 3.35 nM) which led to zero concentration of K252a in the media by DIV28. At DIV 28 the IGF1 and progesterone concentration was reduced by factor, 2.5 and 2, respectively, to proceed to long-term culture conditions of PNs and the surrounding network.

Synaptic functionality

To prove that this culture protocol grows PNs that express functional synapses, we immunostained cultures for pre- and postsynaptic biomarkers of functional synapses including VGCCs, glutamate receptor mGluR1, PSD95, glutamate-decarboxylase GAD65, glycine transporter GlyT2, α-synuclein and bassoon using immunocytochemistry at DIV28. All of these biomarkers were present (Figure 2a), indicating the maturity of both the PNs and the surrounding network. To map the functional activity of the cultured PNs, we performed multielectrode array recordings of E18-derived PNs cultured in a 24-well multielectrode array. These PNs first showed spontaneous bioelectrical activity on DIV11. The spike rate constantly increased from 0.15 ± 0.03 Hz on DIV11 to 2.56 ± 0.59 Hz on DIV21. After DIV28, the spike activity become erratic with long periods of silence, but a frequency of 2.79 ± 0.55 Hz was maintained until DIV63 (Figure 2b). We observed both uniform and highly non-uniform spike intervals and trains with silent periods between bursts and spike frequencies of up-to 140 Hz within the bursts. Exchanging the PN culture media for a media previously used in organotypic brain slice culture [2] at DIV28, prevented the erratic spike activity and stabilized the spike frequency at 6.35 ± 1.85 Hz through DIV63.

Cell-type-specific genetic engineering

To evaluate whether the cultured cells could be genetically manipulated and might show an age-dependency in the transfection efficiency, we performed cell-type-specific genetic engineering by transfecting cells with lentiviral particles that lead to an PN-specific expression of green fluorescence protein (GFP) mediated by the L7 promoter [17,18]. We applied viral particles to dissociated PNs on the day of seeding and detected GFP in PNs with minimal off-target expression (<0.02%) at DIV 3 (Figure 3). At DIV14, 61.5 % of the PN population were GFP positive, and these cells did not differ in dendritic structure from PNs without GFP expression (Figure 3). We observed a stable expression of GFP trough DIV163 (Figure 3). The PN development to maturity was very similar to that *in vivo*, as the fusion phase (E17 - P5 ≈ DIV0 – DIV7), the phase of stellate cells with disoriented dendrites (P5 - P7 ≈ DIV7 – DIV9), as well as the phase of orientation and flattering of the dendritic tree (P7 - P21 ≈ DIV9 – DIV23) were observed (Figure 3). Transfection efficiency was high when lentiviral particles were added to the culture prior to DIV28; however, the transfection efficiency fell progressively and expression was delayed when genetic manipulation was performed later (data not shown).

Use of the PN culture to model PCD

After removing all obstacle to create a stable but very flexible rat Purkinje neuron culture which displays most of the *in vivo* features, we evaluated whether the rat PN culture system could be used to model PCD. We examined whether paraneoplastic Yo antibodies have a pathological effect on thus cultured neurons. We found that anti-Yo antibodies significantly altered the structure of the dendritic arbour of PNs over time. Three hallmarks of anti-Yo treatment were observed within 48 hours after application; a reduction in numbers of dendritic branches per order, branch-order in itself and dendritic length. Anti-Yo reduced the numbers of dendritic branches by half for branch orders 6 to 8 at 48 hours after antibody addition and by half for branch orders 5 to 11 at 96 hours (Figure 4a). The branch-order in itself was reduced under anti-Yo by 30% compare to control (Ctrl: 20; Yo_1: 14, Yo_2: 13) within the first 48 hours. At 48 hours, the average dendritic length for branch orders 4-8 in control culture was 23.0 ± 2.6 µm, whereas that in Yo_1-treated culture was 13.6 ± 1.1 µm, and that in Yo_2-treated culture was 13.8 ± 1.2 µm. This reduction in the dendritic length progressed further at 96 hours (Ctrl 22.0 ± 2.7 µm, Yo_1 13.1 ± 1.2 µm, Yo_2 12.1 ± 1.3 µm) (Figure 4a-b). Taken together, these results show that the present of anti-Yo causes loss of the highly branched dendritic arbour of rat PNs in culture.

Discussion

The present study established a protocol for culture of rat PNs that can be used as a model to unravel pathological mechanisms of neurodegeneration. In contrast to mouse cerebellar culture models, cerebellar culture models from rat tissue need a support layer that provides a healthy environment for PN growth and development. We showed that the older the starting tissue, the more mature the support cell layer had to be to achieve a high PN survival rate. PN survival and dendritic tree development were highly dependent on secreted factors and cell-cell interactions. Paracrine factors such as progesterone, insulin and insulin-like growth factor 1 (IGF1) are important *in vitro* and *in vivo* to ensure PN development and maturity as well as the stability of the surrounding neuronal network [19–21]. Furthermore, the calcium

homeostasis of the neuronal network is a key factor during development [22]. In the cerebellum, calcium-dependent PKC subtypes, activated by synaptic inputs from parallel fibres (granule cells) through glutamate receptors mGluR1/4 trigger functional changes as well as long-term anatomical maturation of the PN dendritic tree [16]. In the presented culture, we detected that the extension and retraction of dendritic branches, and subsequently the stabilisation of existing dendrites through building of synaptic connections as well as of the neuronal calcium homeostasis are keys for PN development and survival. In particular the activity of PKC revealed a strong correlation between development as well as survival and the age of the tissue used to derive the neurons. Minimizing the PKC activity considerably improved survival of PNs that were derived from P10 tissue and improved dendritic tree development in PNs derived from E18 and P0 tissue. These results are indicative of biphasic action of PKC during PN

development. Furthermore, analyses of the PN culture under moderate PKC activity revealed well- developed synapses that were positive for P/Q-VGCC and mGluR1, markers indicative of maturity. Beside the observation of the typical synaptic markers also the results of the electrophysiological recording support that the cultured PNs reaching the state of maturity.

The spontaneous activity of the cultured PNs evaluating using electrophysiological recording was very similar to activities detected i*n vivo* recording with one exception. Depend on anatomical and functional maturity *in vivo* PNs fire spontaneous action potentials at frequencies of about 40–50 Hz with a complex trimodal pattern of tonic firing, bursting, and silent modes [23,24]. In our cultured neurons we observed the same complex trimodal pattern but the spike frequency was only 1/10 at DIV63 in comparison to *in vivo*. This result is not unexpectantly as we recorded from a thin multilayer cell network with an approximately thickness of 50 µm.

The development of functional neurons was very similar in our culture to stages previously characterised *in vivo* [25,26]. We observed the fusion phase (E17-P5), the phase of stellate cells with disoriented dendrites (P5-P7), and orientation and flattering of the dendritic tree (P7-P21). At DIV15, the E18-derived PNs had very complex dendritic arbour structure similar to *in vivo* observations at P12 rats. We were unable to culture functional PNs from rat tissue older than P10 under the optimized conditions. All attempts with tissue of age P28, P60 and P180 failed. This was not unexpected as the genetic engineered GFP positive PNs in culture showed clearly during their development how fast a complex arbour is developed. Given that an isolation of PNs at these late stages is not anymore possible without a total destruction of the dendritic arbour. These neurons can't survive the separation procedure.

Although our culture did not rise from adult aged tissue, we demonstrated the different utilities of the rat PN culture system. We showed that this *in vitro* model system can be used to investigate the pathological mechanisms that cause PCD. We demonstrated that treatment of the culture with sera from PCD patients containing anti-Yo resulted in a similar loss of dendritic

structures as previously reported using organotypic cerebellar slice culture [2]. This finding again confirms the functional and thereby pathological role of anti-Yo in PCD development and progression.

Conclusion

We describe an optimized protocol to culture functional PNs from rat cerebellum that provides a complex and robust system with great experimental flexibility. By creating a multilayer structure and optimizing concentrations of hormones, paracrine factors, and activity regulators (progesterone, insulin, IGF-1, K252a) provided at optimal time points (Fig. 5), this system creates the ideal conditions to grow a balanced cerebellar network in miniature. The long-term stability and neuronal complexity of our culture will facilitate further studies of cell- and network-dependent mechanisms of cerebellar degeneration related to PCD or other cerebellar disorders.

Abbreviations

DIV
days *in vitro*
FBS
foetal bovine serum
PNs
Purkinje neurons
PCD
paraneoplastic cerebellar degeneration
PDL
poly-D-lysine
VGCC

voltage-gated calcium channel

Declarations

ACKNOWLEDGMENTS

The authors thank Y.Ishizuka and C.E.Bramham for providing the E18 cerebellum tissue, C. Elliott for helpful discussions, and the *Molecular Imaging Centre (MIC), where the imaging experiments were performed (Department of Biomedicine and the Faculty of Medicine and Dentistry of University of Bergen).*

AUTHORS' CONTRIBUTIONS

M.S. devised the conceptual framework. I.M.U., T.K., and M.S. planned and performed the experiments and analysed the obtained data sets. H.H. performed the lentivirus construction. The paper was written by M.S. and C.A.V. with editing contributions from all the authors.

FUNDING

T.K was supported by University of Bergen PhD grant #2016/7580-RAKA. The work was additionally funded by grants from HelseVest Norway.

AVAILABILITY OF DATA AND MATERIALS

The datasets generated during and/or analysed during the current study are available from the corresponding author on request.

Ethics approval and consent to participate

All procedures performed in this study involving sera samples of human participants were in accordance with the ethical standards of the institutional and/or national research committee and with the 1964 Helsinki Declaration and its later amendments or comparable ethical standards. The study was approved by the regional ethics Committee of Western-Norway No. 188.05. The sera were stored with the participant written consent at the PND Biobank 133/2015 for the purpose of research and publication. All procedures performed in this study involving Hannover GLAST rat embryonal and postnatal brain tissue were performed according to the National Institutes of Health Guidelines for the Care and Use of Laboratory Animals Norway, approvals #FOTS20135149, FOTS20157494 and FOTS20170001.

Consent for publication

Informed consent to publish research results for the given samples was obtained from all individual participants included in the study when samples were stored at the PND Biobank 133/2015.

Competing interests

The authors declare that they have no competing financial interests.

References

1. Greenlee JE (2013) Treatment of paraneoplastic cerebellar degeneration. Curr Treat Options Neurol 15:185–200
2. Schubert M, Panja D, Haugen M, Bramham CR, Vedeler CA (2014) Paraneoplastic CDR2 and CDR2L antibodies affect Purkinje cell calcium homeostasis. Acta Neuropathol (Berl) 128:835–852
3. Kråkenes T et al (2019) CDR2L Is the Major Yo Antibody Target in Paraneoplastic Cerebellar Degeneration. Ann Neurol 86:316–321
4. Greenlee JE et al (2010) Purkinje cell death after uptake of anti-Yo antibodies in cerebellar slice cultures. J Neuropathol Exp Neurol 69:997–1007
5. Panja D, Vedeler CA, Schubert M (2019) Paraneoplastic cerebellar degeneration: Yo antibody alters mitochondrial calcium buffering capacity. Neuropathol Appl Neurobiol 45:141–156
6. Bugos O, Bhide M, Zilka N (2009) Beyond the rat models of human neurodegenerative disorders. Cell Mol Neurobiol 29:859–869
7. Jacob HJ, Kwitek AE (2002) Rat genetics: attaching physiology and pharmacology to the genome. Nat Rev Genet 3:33–42
8. Drummond E, Wisniewski T (2017) Alzheimer's disease: experimental models and reality. Acta Neuropathol (Berl) 133:155–175
9. Nuber S et al (2013) A progressive dopaminergic phenotype associated with neurotoxic conversion of α-synuclein in BAC-transgenic rats. Brain J Neurol 136:412–432

10. von Hörsten S et al (2003) Transgenic rat model of Huntington's disease. Hum Mol Genet 12:617–624
11. Ellenbroek B, Youn J (2016) Rodent models in neuroscience research: is it a rat race? Dis Model Mech 9:1079–1087
12. Dawson TM, Golde TE, Lagier-Tourenne C (2018) Animal models of neurodegenerative diseases. Nat Neurosci 21:1370–1379
13. Emoto K, Yamashita S, Okada Y (2005) Mechanisms of heat-induced antigen retrieval: does pH or ionic strength of the solution play a role for refolding antigens? J Histochem Cytochem Off J Histochem Soc 53:1311–1321
14. De Bartolo P, Florenzano F, Burello L, Gelfo F, Petrosini L (2015) Activity-dependent structural plasticity of Purkinje cell spines in cerebellar vermis and hemisphere. Brain Struct Funct 220:2895–2904
15. Longair MH, Baker DA, Armstrong JD (2011) Simple Neurite Tracer: open source software for reconstruction, visualization and analysis of neuronal processes. Bioinforma Oxf Engl 27:2453–2454
16. Metzger F, Kapfhammer JP (2003) Protein kinase C: its role in activity-dependent Purkinje cell dendritic development and plasticity. Cerebellum Lond Engl 2:206–214
17. Hirai H (2012) Basic research on cerebellar gene therapy using lentiviral vectors. Cerebellum Lond Engl 11:443–445
18. Nitta K, Matsuzaki Y, Konno A, Hirai H (2017) Minimal Purkinje Cell-Specific PCP2/L7 Promoter Virally Available for Rodents and Non-human Primates. Mol Ther Methods Clin Dev 6:159–170
19. Wessel L et al (2014) Long-term incubation with mifepristone (MLTI) increases the spine density in developing Purkinje cells: new insights into progesterone receptor mechanisms. Cell Mol Life Sci CMLS 71:1723–1740
20. Croci L et al (2011) Local insulin-like growth factor I expression is essential for Purkinje neuron survival at birth. Cell Death Differ 18:48–59
21. Hami J et al (2016) Stereological study of the effects of maternal diabetes on cerebellar cortex development in rat. Metab Brain Dis 31:643–652
22. Metzger F (2010) Molecular and cellular control of dendrite maturation during brain development. Curr Mol Pharmacol 3:1–11
23. Armstrong DM, Rawson JA (1979) Activity patterns of cerebellar cortical neurones and climbing fibre afferents in the awake cat. J Physiol 289:425–448
24. Womack M, Khodakhah K (2002) Active Contribution of Dendrites to the Tonic and Trimodal Patterns of Activity in Cerebellar Purkinje Neurons. J Neurosci 22:10603–10612
25. McKay BE, Turner RW (2005) Physiological and morphological development of the rat cerebellar Purkinje cell: Purkinje cell output parallels dendritic development. J Physiol 567:829–850
26. Kapfhammer JP (2004) Cellular and molecular control of dendritic growth and development of cerebellar Purkinje cells. Prog Histochem Cytochem 39:131–182

Tables

Table 1 | Primary antibodies. The signal to noise ratio for the antibodies were evaluated for the following conditions: 4% PFA at pH 7.2 diluted in 100 mM PBS; 1.5% PFA at pH 6 diluted in 100mM natrium acetate buffer (NaAcB)); without heat-induced antigen retrieval (HIAGR); and with HIAGR either TRIS-based (pH 9) or citric acid-based (pH 6). The best conditions for each used antibody are described below.

Antibody	Species	Company	Cat. No.	LOT No.	RRID	Dilution [µg/mL]	PFA fixation	HIAGR	Marker
A-Synuclein	chicken	EnCorBio	CPCA-SNCA	71113	AB_2572385	1.0	1.5%; pH 6; NaAcB	No	Pre-synapse, granule and unipolar brush cells /PNs
Bassoon	chicken	SYSY	141016	141016/1-1	AB_2661779	Serum 1:500	4%, pH 7.2; PBS	No	Pre-synapse; Golgi / granule cells, or basket cells / PNs
Calbindin	guinea pig	SYSY	214005	214005/1-5	AB_2619902	0.5	4%, pH 7.2; PBS	No	Purkinje neurons
	chicken	SYSY	214006	214006/1-3	AB_2619903	Serum 1:750	4%, pH 7.2; PBS	No	Purkinje neurons
Calretinin	chicken	SYSY	214106	214106/2	AB_2619909	Serum 1:500	4%, pH 7.2; PBS	No	Unipolar-brush cells
CNP1	rabbit	SYSY	355003	355003/1-2	AB_2620112	1.0	4%, pH 7.2; PBS	No	Oligodendrocytes
$GABA_AR\alpha6$	rabbit	SYSY	224603	224603/3	AB_2619945	5.0	4%, pH 7.2; PBS	pH 9	Granule cells
GAD65	mouse	BD Bio-science	559931	4283665	AB_397380	2.5	1.5%; pH 6; NaAcB	No	Pre-synapse, stellate and basket cells / PNs
GlyT2	guinea pig	SYSY	272004	27004/2	AB_2619998	Serum 1:250	4%, pH 7.2; PBS	pH 6	Golgi cells; Lugaro cells
IBA1	rabbit	EnCorBio	RPCA-IBA1	266_100517	AB_2722747	1.0	4%, pH 7.2; PBS	No	microglia
mGluR1	guinea pig	FRONTIER	2571801		AB_2571801	2.5	1.5%; pH 6; NaAcB	No	PNs, Lugaro cells
Neurogranin	rabbit	SYSY	357003	357003/1	AB_2620115	2.5	4%, pH 7.2; PBS	No	Golgi cells
Parvalbumin	guinea pig	SYSY	195004	195004/1-21	AB_2156476	Serum 1:500	4%, pH 7.2; PBS	No	PNs, basket and stellate cells
PCP2	rabbit	Takara	M194	1AFXJ002.0		1.0	4%, pH 7.2; PBS	No	Purkinje neurons
Peripherin	rabbit	EnCor Bio	RPCA-Peri	0208_070316	AB_2572375	0.5	4%, pH 7.2; PBS	No	Mossy and climbing fibers
PSD95	mouse	Neuro mab	75-028	455.7JD.22G	AB_2292909	5.0	1.5%; pH 6; NaAcB	No	Post-synapse
Synapsin 1/2	chicken	SYSY	106006	106006/1-4	AB_2622240	Serum 1:500	1.5%; pH 6; NaAcB	No	Pre-synapse
VGCC-PQ α-1A	guinea pig	SYSY	152205	152205/3	AB_2619842	4.0	1.5%; pH 6; NaAcB	No	Purkinje neuron synapse
VGluT2	guinea	SYSY	135404	135404/2-32	AB_887884	Serum	4%, pH	pH 6	Mossy and

	pig	1:500	7.2; PBS	climbing fibers

EnCorBio: EnCor Biotechnology; SYSY: synaptic systems; PN: Purkinje neuron

Figures

Figure 1

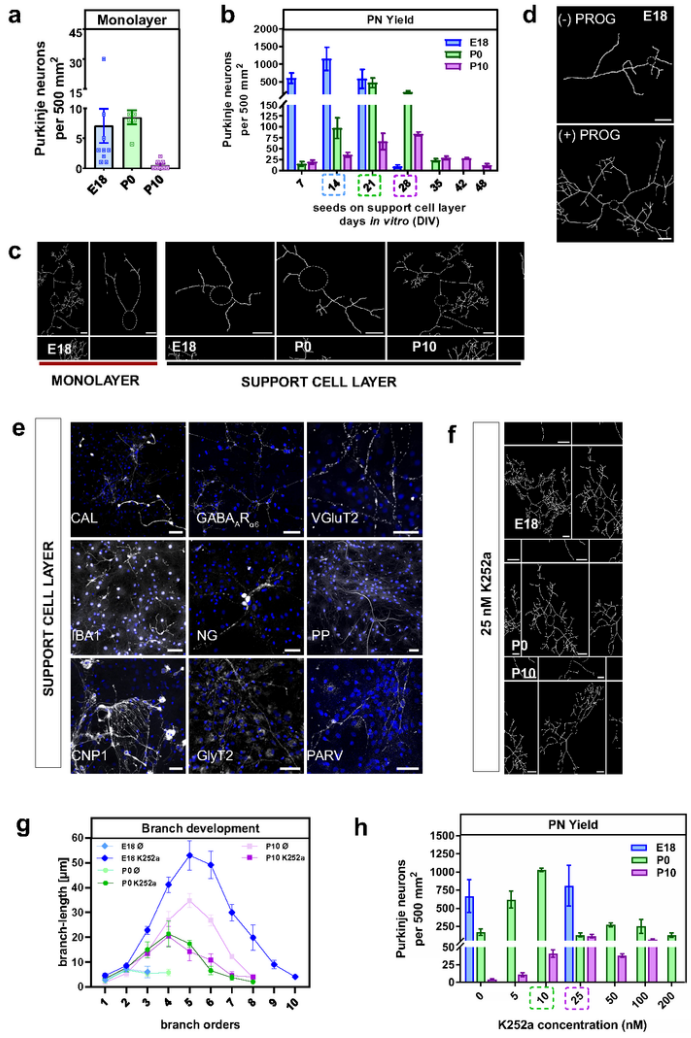

Figure 1

Optimization of rat PN culture. (**a**) PN yield in a monolayer on PDL-laminin-coated coversilps at DIV 28 for PN derives from rat cerebelli of indicated ages; (**b**) Yields of E18-, P0- and P10-derived PNs as a function of age of the support cell layer. (**c**) Representative PN skeletons for E18-derived PNs as a monolyer, and E18-, P0-, and P10-derived PNs on a support cell layer. Scale bars, 20 µm; (**d**) Representative skeletons of E18-derived PNs cultured without and with 40 µM progesterone on dendritic branching. Scale bars, 20 µm; (**e**) Images of support cell layer stained for major cell types (white): unipolar brush cells (stained for calretinin (CAL)), granule cells (stained for GABAARα6), Golgi cells (stained for NG-neurogranin, and GlyT2), Lugaro cells (stained for GlyT2), stellate and basket cells (stained for parvalbumin (PAV)), mossy and climbing fibres (stained for VGluT2 and peripherin (PP)), oligodendrocytes (stained for CNP1), and microglia (stained for IBA1). Nuclei were stained with DAPI (blue). Scale bars, 50 µm. (**f**) Representative PN skeletons dependent on derived neuron age and protein kinase C (PKC) antagonist K252a. Scale bars, 20 µm; (**g**) Dendritic branch length versus branch orders for PNs derived from E18, P0, and P10 tissue without and with 25 µM K252a. (**h**) of PN yield at indicated K252a concentration for E18-, P0-, and P10-derived PNs.

Figure 2

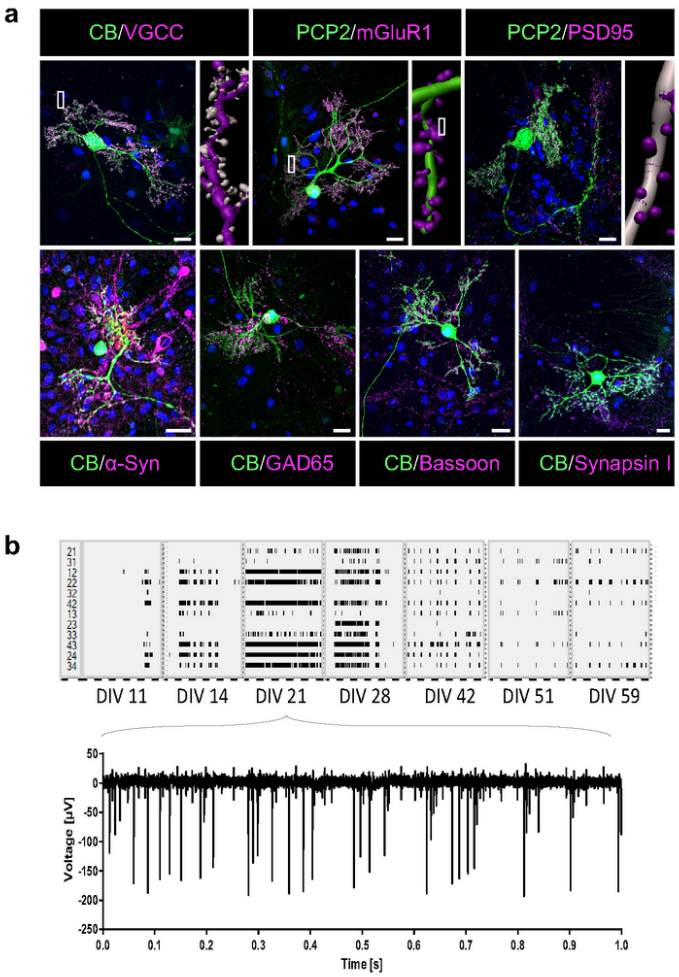

Figure 2

Cultured rat PNs are functional (**a**) Representative images of cultured PNs (green, calbindin (CB) or Purkinje cell specific protein 2 (PCP2)) stained (magenta) for post-synaptic biomarker VGCC, mGluR1, and PSD95, and presynaptic biomarkers α-synuclein (α-syn, marker of glutamatergic synaptic terminals from granule cells (parallel fibres) and unipolar brush cells (type I/II)), GAD65 (marker of axon terminals from stellate and basket cells), bassoon (marker of the active zone of mossy fibre terminals and parallel fibre terminals between Golgi cells and granule cells, and between basket cells and Purkinje neurons), and synapsin I (synaptic vesicle phosphoprotein of mature CNS synapses). Nuclei were stained with DAPI (blue). In each image, the 3D IMARIS cartoon reconstruction of a protein-positive synapse is shown for on PN dendrite. Scale bars, 20 µm. (**b**) Micro-electrode array spike patterns (10 s) of E18-derived PNs cultured in a 24-well multielectrode array plate at indicated DIVs with an enlarged view (1s) at DIV21.

Figure 3

Rat PNs in culture can be genetically manipulated: Live-cell imaging of E18-derived PNs expressing lentiviral-induced GFP from day of seeding (DIV0) through DIV53. Scale bars, 50 µm.

Figure 4

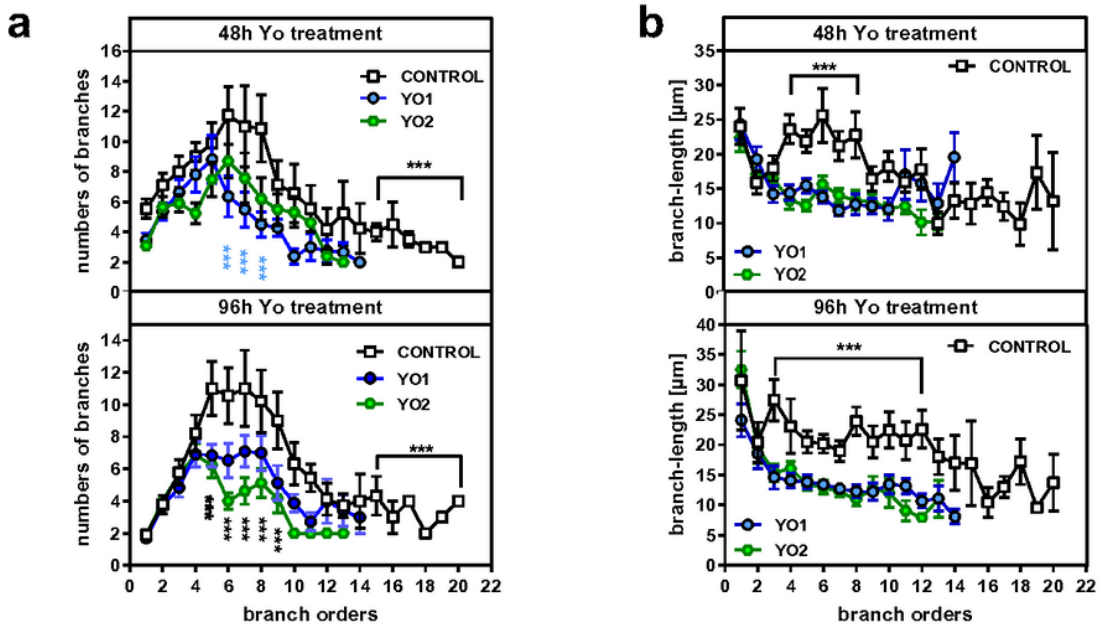

Figure 4

PN pathology induced by PCD antibody Yo. (**a**) Comparison of numbers of branches of treated PNs between serum from healthy volunteers and sera containing anti-Yo at 48 hours (upper-graph) and 96 hours (lower graph). (**b**) Time-dependent comparison of branch order versus dendritic length for control and anti-Yo-treated PN culture.

Figure 5

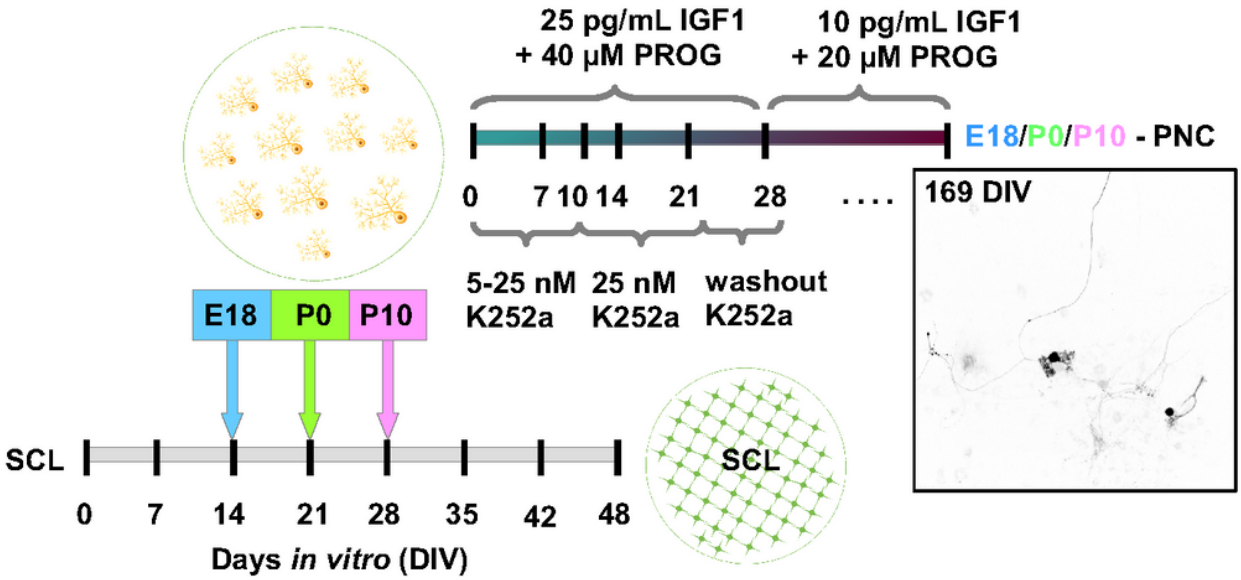

Figure 5

Optimized multilayer rat PN culture protocol. Each age-tissue-dependent culture required different conditions of support and activity regulation. The supplementation with insulin-like growth factor 1 (IGF1) and progesterone (PROG) provided a stable environment resulting in high PN survival rates. PKC activity modulation shaped the dendritic tree development of E18- and P0-derived culture; for P10-derived culture, survival was highly dependent on the inhibition of PKC but dendritic tree development was not. The protocol can be used to grow stable PN cultures for up to 6 months (DIV163) in a 6- to 24-well format.